

Scattering quantum random-walk search with errors

A. Gábris,¹ T. Kiss,¹ and I. Jex²

¹ Research Institute for Solid State Physics and Optics, H-1525 Budapest, P. O. Box 49, Hungary

² Department of Physics, FJFI ČVUT, Břehová 7, 115 19 Praha 1 - Staré Město, Czech Republic

(Dated: December 20, 2018)

We analyze the realization of a quantum-walk search algorithm in a passive, linear optical network. The specific model enables us to consider the effect of realistic sources of noise and losses on the search efficiency. Photon loss uniform in all directions is shown to lead to the rescaling of search time. Deviation from directional uniformity leads to the enhancement of the search efficiency compared to uniform loss with the same average. In certain cases even increasing loss in some of the directions can improve search efficiency. Phase noise modifies the time-dependent oscillation of success probability resulting in damped oscillation on average that asymptotically tends to a non-zero value.

I. INTRODUCTION

The generalization of random walks for quantum systems [1] proved to be a fruitful concept [2] attracting much recent interest. Algorithmic application for quantum information processing is an especially promising area of utilization of quantum random walks (QRW) [3].

In the pioneering work [4] Grover designed a quantum search algorithm which scales with the square root of the number of items, instead of linear scaling as in classical searches. Shenvi, Kempe and Whaley (SKW) [5] proposed a search algorithm based on quantum random walk on a hypercube, which has the same scaling properties. In their algorithm they use the oracle to modify the quantum coin at the marked node. In contrast to the Grover search, this algorithm has to be repeated several times to succeed, but this merely adds an overhead independent of the size of the search space.

There is a variety of suggestions and some experiments to realize quantum walks in a laboratory. In general, it is possible to design scalable networks made of controlled NOT gates and one qubit rotations to realize QRWs, thereby utilizing any implementation of such gates [6]. The schemes proposed to directly implement QRWs include ion traps [7], nuclear magnetic resonance [8] which was also experimentally verified [9], cavity quantum electrodynamics [10, 11], optical lattices [12], optical traps [13], optical cavity [14], and classical optics [15].

The idea of the scattering random walk (SQRW) [16] was proposed as an answer to the question: how to realize a coined walk by a quantum optical network built from passive, linear optical elements such as beam splitters and phase shifters? It turned out that such a realization is possible and, in fact, it leads to a natural generalization of the coined walk, the scattering quantum random walk [17]. The SQRW on the hypercube allows for a quantum optical realization of the search algorithm of the SKW algorithm [5]. Having a proposal for a physical realization at hand one can discuss the effects hindering successful operation.

Noise and decoherence strongly influence quantum walks, for a recent review see Ref. [18]. The first investigations of decoherence indicated that a small amount

of decoherence can actually enhance the mixing property [19]. For a continuous QRW on a hypercube there is a threshold for decoherence, beyond which the walk behaves like a classical one [20]. Košík *et al* analyzed SQRW with randomized phase noise on a d dimensional lattice [21]. The quantum random walk search with imperfect gates was discussed in some detail by Li *et al* [22]. Their assumption was that the Grover operator applied in the search is modified by a random phase. Such an imperfection decreases the search probability and also shifts its first maximum in time.

In this paper, we consider different types of noise affecting the SQRW search algorithm. In particular, we focus on non-uniform (direction dependent) losses and show that somewhat contradicting to naïve expectation this can lead to non-trivial effects, such as to the enhancement of the search efficiency. As a second type of errors we study randomly distributed phase disturbances, which are fixed for each run of the search algorithm. This type of phase errors has not yet been considered in the literature. We show also that in this case interesting effects can be found. The average search probability displays a damped oscillatory behaviour and asymptotically tends to a non-zero constant value.

The paper is organized as follows. In the next section we introduce the scattering quantum walk search algorithm. In section III. we derive analytic results for the success probability of search for the case when a uniform constant describes photon losses. In section IV. we turn to direction dependent losses, show numerical results and give an estimation for the success probability of the search. In section V. phase noise is considered and consequences for the success probability is worked out.

II. THE SCATTERING QUANTUM WALK SEARCH ALGORITHM

The quantum walk search algorithm is based on a generalized notion of coined quantum random walk (CQRW) according to which the coin flipping operator may be different for different nodes. The CQRW is defined on the product Hilbert space $\mathcal{H} = \mathcal{H}^C \otimes \mathcal{H}^G$, where \mathcal{H}^C refers to

the quantum coin, and \mathcal{H}^G represents the graph on which the walker is moving around. The discrete time-evolution of the system is governed by the unitary operator

$$U = SC, \quad (1)$$

where C is the coin operator which corresponds to flipping the quantum coin, and S is the step or translation operator that moves the walker one step along some outgoing edge, depending on the coin state. According to the original definition, C is position (node) independent and thus acts as the identity on \mathcal{H}^G . Adopting a binary string representation of the vertices V of underlying graph $G = (V, E)$, the step operator S , which is a permutation operator of the entire Hilbert space \mathcal{H} , can be expressed as

$$S = \sum_{d=0}^{n-1} \sum_{x \in G} |d, x \oplus e_{dx}\rangle \langle d, x|. \quad (2)$$

In Eq. (2) x stands for the indices of nodes in the graph, and d is the index of a direction in which it is possible to leave the node x . Further, e_{dx} represents the edge connecting x to the next node in the direction d .

To define the scattering quantum random walk on an n regular graph of N nodes, we consider an array of similar n -multiports arranged in columns (each containing N multiports) enumerated from left to right. We assume the initial state to enter the input ports on the left hand side, and using an appropriate labelling of input and output ports, we connect each output of a multiport in column j to some multiport in the next column $j + 1$ according to the graph.

The labelling most suitable for representing the quantum walk is the following. We label a given mode by the row number and input port number of the multiport it is connected to, hence we write it as $|d, x\rangle$, where $d = 0, 1, \dots, n - 1$ labels the input ports and $x = 0, 1, \dots, N - 1$ stands for the row number. Thus we have essentially separated the total Hilbert space into a product $\mathcal{H}^C \otimes \mathcal{H}^G$. The column labels can be thought of as time steps, and as it will be shown shortly, the time-evolution $U = SC$ is generated by propagation through columns of multiports.

To proceed, we recall the effect of an n multiport on an arbitrary single excitation incoming state (e.g. in \mathcal{H}^C). The $SU(n)$ transformation matrix \mathbf{C} is given by the formula

$$\sum_{d=0}^{n-1} a_d |d\rangle \rightarrow \sum_{d,k=0}^{n-1} C_{dk} a_k |d\rangle, \quad (3)$$

where $|d\rangle$ denotes the state where the photon is in the d mode, i.e. $|d\rangle = |0\rangle_0 \dots |1\rangle_d \dots |0\rangle_{N-1}$. According to the original definition, we assume that it is possible to choose a labelling of output and input ports such that the output port labels and the input port labels coincide for each connection prescribed by the vertices in V . This

is an important assumption to be able to show that the SQRW is a superset of the generalized CQRW, however, it is not a necessary restriction for the SQRW.

The transformation realized by a row of similar multiports connected to the next row such that the output port d of the multiport x in the first row is connected to the input port d of $x \oplus e_{dx}$ in the next row, is therefore given by

$$\sum_{d,x} a_{dx} |d, x\rangle \rightarrow \sum_{dkx} C_{dk} a_{kx} |d, x \oplus e_{dx}\rangle. \quad (4)$$

Using Eqs. (2) and (3) one can verify that this formula exactly corresponds to the $U = SC = S(C_0 \otimes \mathbb{1})$ transformation where C_0 is generated by the matrix \mathbf{C} of the multiports. Since the coin operation C is realized locally by the multiports at each node, it is straight-forward to realize position dependent coin operations, such as that required for the quantum walk search algorithm.

The SKW algorithm [5] is based on application of two distinct coin operators

$$C_0 = G \quad (5)$$

$$C_1 = -\mathbb{1}, \quad (6)$$

where G is the Grover inversion or diffusion operator. The application of the two coin operators is conditioned on the result of oracle operator \mathcal{O} . The oracle marks one x_t as target, hence the coin operator is conditioned on the node:

$$C' = C_0 \otimes \mathbb{1} + (C_1 - C_0) \otimes |x_t\rangle \langle x_t|. \quad (7)$$

When n is large, the operator $U' := SC'$ can be regarded as a perturbed variation of $U = S(C_0 \otimes \mathbb{1})$. As mentioned, the conditional transformation (7) is very simple to implement in the multiport network. For this particular case one has to use a simple phase shifter at position x_t in every column of the array, and a multiport realizing the Grover matrix G at every other position. The connection topology required to implement a walk on the hypercube is such that in the binary representation we have $e_d = 0 \dots 1 \dots 0$ with 1 being at the d 'th position, i.e. $e_d = 2^d$.

Of course, for practical implementations, using an additional column of N multiports for every time step is unpractical, and one would rather feed the outputs into the appropriate inputs of the same column. This setup then becomes similar to the one introduced in Ref. [17].

III. UNIFORM DECAY

We begin the analysis of effect of errors on the quantum walk search algorithm with the discussion of photon losses. In such an optical network this type of error is unavoidable, and especially for single excitation initial states, it is also very straight-forward to describe.

The simplest case is when all arms of the involved multiports suffer the same losses. Let this loss rate be characterized by the transmission coefficient η , such that the operator that describes the effect of decay on a single excitation density operator can be expressed as

$$\mathcal{D}(\varrho) = \eta^2 \varrho + (1 - \eta^2) |0\rangle\langle 0|. \quad (8)$$

Hence, the total evolution of the system after one iteration may be written as $\varrho \rightarrow \mathcal{D}(U\varrho U^\dagger)$. It is important to notice that with the introduction of this error, we leave the originally defined search space \mathcal{H}^G , thus the QRW evolution operator U must also be extended. The extension $U|0\rangle = |0\rangle$ is trivially provided by our physical implementation, and it will always be implied in the following. Due to the nature of Eq. (8) and the extension of U , one can see that the order of applying the unitary time step and the error operator \mathcal{D} can be interchanged. Therefore, over t steps the state of the system undergoes the transformation

$$\varrho \rightarrow \eta^{2t} U^t \varrho U^{\dagger t} + (1 - \eta^{2t}) |0\rangle\langle 0| = \mathcal{D}^t(U^t \varrho U^{\dagger t}). \quad (9)$$

To simplify further calculations, we introduce a linear (but non-unitary) operator to denote the effect of the noise operator \mathcal{D} on the search Hilbert space:

$$D|\psi\rangle = \eta|\psi\rangle. \quad (10)$$

This operator is just a multiplication and hence obviously linear, however, for $\eta < 1$ it is non-unitary. We can also deduce that it does not include any coherence damping within the one-photon subspace, since it only uniformly decreases the amplitude of the computational states (at the expense of introducing vacuum to the system). Since all final statistics are gathered from the search Hilbert space \mathcal{H}^G , it is possible to drop the vacuum from all calculations, and incorporate all information related to it into the norm of the remaining state. In other words, we can think of DU as the time step operator, and relax the requirement of normalization. Using this notation, the effect of t steps is very straight-forward to express:

$$|\psi\rangle \rightarrow \eta^t U^t |\psi\rangle. \quad (11)$$

This formula indicates that inclusion of the effect of uniform loss may be postponed until just before the final measurement. Hence, it might simply be included in the detector efficiency (as an exponential function of the number of iterations).

Applying this model of decay to the quantum walk search algorithm we can define the new step operator $U'' = DU'$. Using the above notations, after t steps the final state of the system can be written as

$$(U'')^t |\psi_0\rangle = \eta^t \cos \omega'_0 t |\psi_0\rangle - \eta^t \sin \omega'_0 t |\psi_1\rangle + \eta^t O\left(\frac{n^{3/4}}{\sqrt{2^n}}\right) |\tilde{r}\rangle \quad (12)$$

Adopting the notation of Ref. [5], the probability of measuring the target state $|x=0\rangle$ in the output state after t steps can be expressed as

$$\begin{aligned} p(t) &= \sum_{d=0}^{n-1} |\langle d, 0 | (U'')^t \psi_0 \rangle|^2 \\ &= \eta^{2t} \sin^2 \omega'_0 t |\langle R, 0 | \psi_1 \rangle|^2 + 1/2^n \eta^{2t} \cos^2 \omega'_0 t \\ &\quad + O(1/2^n). \end{aligned} \quad (13)$$

We know from Ref. [5] that $|\langle R, 0 | \psi_1 \rangle|^2 = 1/2 - O(1/n)$, also because of the $1/2^n$ factor, the second term can be omitted as long as the sin term is non-vanishing, which is going to be the case. Therefore for large n it is sufficient to maximize the following function:

$$p(t) = \eta^{2t} \sin^2 \omega'_0 t (1/2 - O(1/n)). \quad (14)$$

The search for the maximum yields:

$$\tan(\omega'_0 t_f) = \frac{\omega'_0}{-\ln \eta}, \quad (15)$$

$$\tan(2|\omega'_0|t_f) < \tan(|\omega'_0|t_f) = \frac{|\omega'_0|}{-\ln \eta}. \quad (16)$$

Since we expect an overall exponential drop of probability due to the η^{2t} factor, we expect the maximum to be before the ideal time-point $|\omega'_0|t = \pi/2$. Therefore, we can restrict the condition (16) to $\pi/4 < |\omega'_0|t \leq \pi/2$. The boundaries also give some indication of the validity of dropping the cos term from Eq. (13): when the maximum is found outside of $\pi/4 < |\omega'_0|t \leq \pi/2$, then dropping this term is not justified.

Again using results from Ref. [5] we have $|\omega'_0| = 1/\sqrt{2^{n-1}}[1 - O(1/n)] \pm O(n^{3/2}/2^n)$, of which the last term can be dropped. Substituting this into (15) and expressing the maximum time we get $t_f = \sqrt{2^{n-1}} \left[\text{acot}(-\ln \eta \sqrt{2^{n-1}}) + O(1/n) \right]$. Therefore we decide to take

$$t_m := \sqrt{2^{n-1}} \text{acot}(-\ln \eta \sqrt{2^{n-1}}), \quad (17)$$

or the closest integer during operation.

To simplify the following calculations, we introduce the following new variables

$$x = -\ln \eta \sqrt{2^{n-1}}, \quad (18)$$

$$\eta = 1 - 2^{-\epsilon}, \quad (19)$$

where ϵ can be regarded as some logarithmic noise parameter, i. e. the ideal case corresponds to $\epsilon = \infty$, while complete attenuation is $\epsilon = 0$. When epsilon is sufficiently large, the expression $-\ln \eta$ can be approximated to first order in $2^{-\epsilon}$ and we obtain

$$x \approx 2^{-\epsilon + n/2 - 1/2}. \quad (20)$$

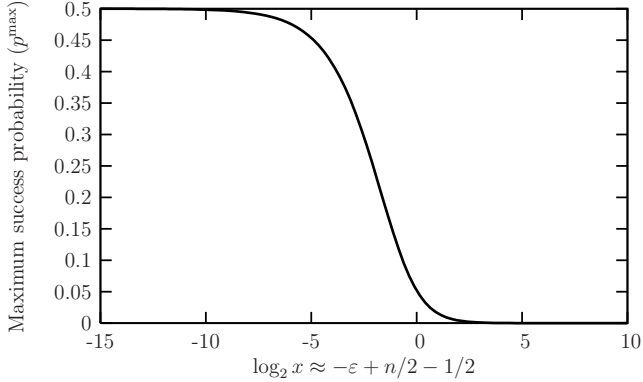


FIG. 1: Probability of measuring the target state after the optimal number of iterations according to the approximation in Eq. (23). The probability is plotted against the logarithm of x which is a combination of the rank of the hypercube n and the logarithmic transmission parameter ε .

We use (14) to obtain the probability at time t_m . Using the new variable x , we can express the sine term as

$$\begin{aligned} \sin^2 \omega'_0 t_m &= \sin^2 |\omega'_0| t_m = \sin^2 [\operatorname{acot} x (1 + O(1/n))] = \\ &= \frac{1}{1+x^2} + \frac{2x \operatorname{acot} x}{1+x^2} O(1/n) + \frac{\operatorname{acot}^2 x}{1+x^2} O(1/n^2), \end{aligned} \quad (21)$$

and then for the maximum success probability $p^{\max}(\eta) = p(t_m)$ we obtain

$$p^{\max}(\eta) = \frac{e^{-2x \operatorname{acot} x}}{1+x^2} \left[\frac{1}{2} - O(1/n) + x \operatorname{acot} x O(1/n) \right]. \quad (22)$$

For large n it depends on n and η only in the combination in x , hence we can write

$$p^{\max}(x) \approx \frac{1}{2} \exp(-2x \operatorname{acot} x) \frac{1}{1+x^2}. \quad (23)$$

This function is plotted on Fig. 1. On Fig. 2 the theoretical approximations (drawn with continuous lines of different patterns) can be compared to the results of numerical calculations represented by connected points with the same line pattern as the corresponding approximates. In comparison with the ideal case, a different behaviour of the approximative values can be observed at lower transmission rates, e.g. at $\varepsilon = 2$ which case is included on Fig. 2. As it was shown in Ref. [5], $1/2$ is always an upper bound on the actual success probability with an accuracy of $O(1/n)$. However, in the non-ideal case, the approximation is not an upper bound any more, and $O(1/n)$ deviations can be expected to either direction. The quantitative analysis of the sign of the correction term is beyond the scope of the present paper. What we expect from Eq. (22) is that the positive contribution becomes more significant for large x , hence for small values of ε for some fixed n . This is confirmed by the plots on Fig. 2.

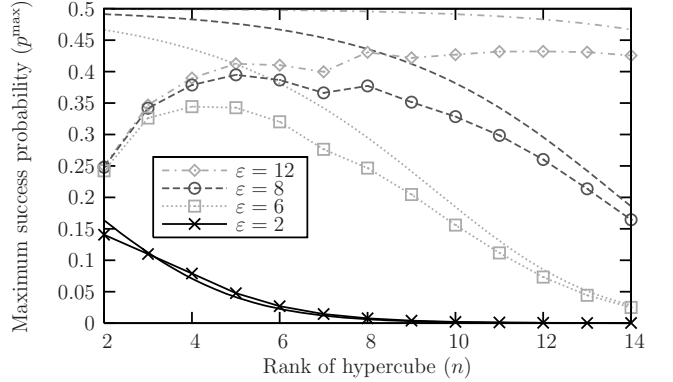


FIG. 2: Approximated and numerically calculated maximum success probabilities for different ranks of hypercube (n). The theoretical approximations are drawn with continuous curves and the results of numerical calculations are presented as connected points. The approximated and calculated results for similar logarithmic transmission parameters ε are plotted with the same line patterns and colours.

IV. DIRECTION DEPENDENT LOSS

The assumption that all the optical paths have the same loss rates might not hold in every realization. It can easily happen for instance that different loss rates are associated with each optical path. In the present section we use the underlying symmetry of the hypercube implementation and assume that modes originating from the same ports of multiports have similar loss characteristics. The operator \mathcal{D} describing this decoherence mechanism acts on a general term of the density operator as

$$\mathcal{D}(|d, x\rangle \langle d', x'|) = \eta_d \eta_{d'} |d, x\rangle \langle d', x'| + \delta_{xx'} \delta_{dd'} \eta_d^2 |0\rangle \langle 0|. \quad (24)$$

To describe the overall effect of this operator on a pure state, we re-introduce the linear decoherence operator in a more general form,

$$D = \sum_d \eta_d |d\rangle \langle d| \otimes \mathbb{1}, \quad (25)$$

and introduce the notation $\{\eta\}$ to denote the set of coefficients η_d . Due to the symmetry of the system the sequential order of coefficients is irrelevant. With this re-defined operator the effect of decoherence can be written

$$\mathcal{D}(\varrho) = \varrho' + (1 - \operatorname{Tr} \varrho') |0\rangle \langle 0|, \quad (26)$$

where $\varrho = |\psi\rangle \langle \psi|$ is the initial state, and the non-vacuum part of the output state is $\varrho' = |\psi'\rangle \langle \psi'|$, with $|\psi'\rangle = D|\psi\rangle$. Therefore, we can again reduce our problem to calculating the evolution of unnormalized pure states, just as in the uniform case, and we can use the non-unitary step operator $U'' = DU'$ with the more general noise operator.

Telling how well the algorithm performs under these conditions is a complex task. First we give a lower bound

on the probability of measuring the target node, based on generic assumptions. To begin we separate the noise operator into two parts

$$D = \eta + D', \quad (27)$$

where for the moment we leave $0 \leq \eta \leq 1$ undefined. It follows from (25) that the diagonal elements of D' are $[D']_{dd} = \delta_d = \eta_d - \eta$, and the off-diagonal elements are zero. From Eq. (26) it follows that starting from a pure state $|\psi_0\rangle$, after t non-ideal steps the state of the system can be characterized by the unnormalized vector $|\psi'(t)\rangle$, which is related to the state of the same system after t ideal steps as

$$|\psi'(t)\rangle = \eta^t |\psi(t)\rangle + |r\rangle. \quad (28)$$

The residual vector $|r\rangle$ can be expressed as

$$|r\rangle = \sum_{k=1}^t (DU')^{t-k} D' \eta^{k-1} |\psi(k)\rangle. \quad (29)$$

To obtain the probability of measuring the target state $|x=0\rangle$ we have to evaluate the formula

$$p(t) = \sum_{d=0}^{n-1} |\eta^t \langle d, 0 | \psi(t) \rangle + \langle d, 0 | r \rangle|^2. \quad (30)$$

Due to the symmetry of the graph and the coins, we use e. g. Eq. (14) and obtain $\langle d, 0 | \psi(t) \rangle \approx -\sin(\omega_0' t)/\sqrt{2n}$. To obtain a lower bound on $p(t)$ we note that the sum is minimal if $\langle d, 0 | r \rangle = \text{const} = K$ for every d (we consider a worst case scenario when all $\langle d, 0 | r \rangle$ are negative). From now on we assume that the second term is a correction that's absolute value is smaller than that of the first term. We shall return later to the case when this assumption is not valid. When this is case, we first search for an upper bound on K , and we use the inequality

$$\sum_{d=0}^{n-1} |\langle d, 0 | r \rangle|^2 \leq \langle r | r \rangle \quad (31)$$

to achieve this. The norm of $|r\rangle$ can be bound using the eigenvalues of U , D , and D' . Let $\eta_{\max} = \max\{\eta_d | d = 0, \dots, n-1\}$ and $\delta_{\max} = \max\{|\delta_d| | d = 0, \dots, n-1\}$. Then we have

$$\langle r | r \rangle \leq \sum_{k=1}^t \eta_{\max}^{t-k} \delta_{\max} \eta^{k-1} = \frac{\eta_{\max}}{\eta} \frac{\delta_{\max}}{\eta_{\max} - \eta} (\eta_{\max}^t - \eta^t). \quad (32)$$

Since U is unitary, its contribution to the above formula is trivial. Our upper bound on $|K|$ hence becomes $|K| \leq 1/\sqrt{n}(\eta_{\max} \delta_{\max} / \eta)(\eta_{\max}^t - \eta^t) / (\eta_{\max} - \eta)$. Putting the results together, we obtain a lower bound on the probability for measuring the target node,

$$p(t) \geq \eta^{2t} \left\{ \sqrt{p_i(t)} - \frac{\eta_{\max}}{\eta} \frac{\delta_{\max}}{\eta_{\max} - \eta} \left[\left(\frac{\eta_{\max}}{\eta} \right)^t - 1 \right] \right\}^2, \quad (33)$$

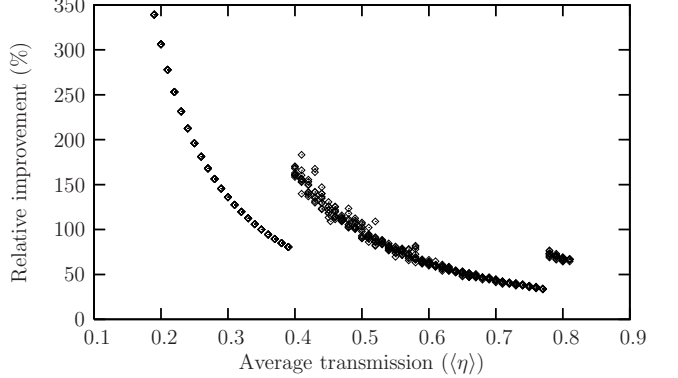


FIG. 3: The relative improvement of success probability $[p^{\max}(\{\eta\}) - p^{\max}(\langle \eta \rangle)]/p^{\max}(\langle \eta \rangle)$ which compares direction dependent loss to uniform loss. The transmission coefficient of the uniform loss is the average $\langle \eta \rangle$ of the distribution $\{\eta\}$. The points are generated for $Q = 0.35$ and in the entire available domain for $\langle \eta \rangle$. The higher moments of $\{\eta\}$ are not restricted therefore we see multiple values for certain $(\langle \eta \rangle, Q)$ pairs. (Rank of hypercube $n = 9$.)

where $p_i(t)$ stands for the corresponding probability for the ideal (lossless) case. The lower bound can be made the strongest by maximizing it with respect to the arbitrary parameter η . This procedure can be carried out noting that $\delta_{\max} = \max\{\eta_{\max} - \eta, \eta - \eta_{\min}\}$, and it gives the maximum at $\bar{\eta} = (\eta_{\max} + \eta_{\min})/2$, yielding the formula

$$p(t) \geq \bar{\eta}^{2t} \left\{ \sqrt{p_i(t)} - (\eta_{\max}/\bar{\eta}) \left[(\eta_{\max}/\bar{\eta})^t - 1 \right] \right\}^2. \quad (34)$$

We note that Eq. (33) and hence Eq. (34) is only valid under the assumption that the correction term is smaller than $\sqrt{p_i(t)}$. When this assumption breaks down, we opt to set the lower bound to zero.

These generic assumptions brought us to the conclusion that the transmission rate that governs the damping is $\bar{\eta}$ which is the average of the highest and lowest transmission coefficients. A different approach to study the behaviour of the maximum success probability reveals the importance of another average which is the mean value of the set $\{\eta\}$,

$$\langle \eta \rangle = 1/n \sum_{d=0}^{n-1} \eta_d. \quad (35)$$

To see this we consider the Taylor expansion of $p^{\max}(\{\eta\})$ around $\eta_d = \langle \eta \rangle$ ($d = 0, \dots, n-1$). With using the permutation symmetry of $p^{\max}(\{\eta\})$, and $\sum_k \delta_k = 0$ which is due to the special choice of the point of expansion, we arrive at

$$p^{\max}(\{\eta\}) = p^{\max}(\langle \eta \rangle) + B/n \sum_{k=0}^{n-1} \delta_k^2 + C/n \sum_{k=0}^{n-1} \delta_k^3 + R. \quad (36)$$

For simplicity, we introduce the notations $Q^2 = 1/n \sum_k \delta_k^2$ and $W^3 = 1/n \sum_k \delta_k^3$. Q may be regarded as

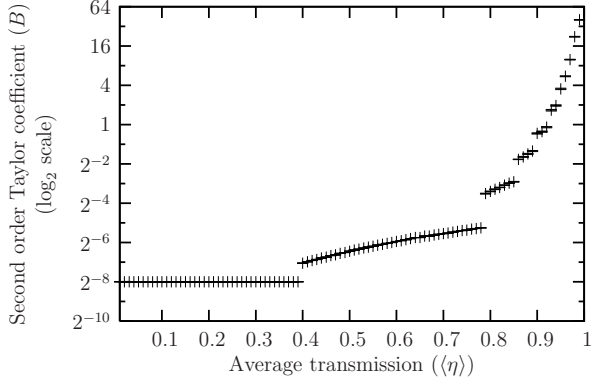


FIG. 4: The coefficients for the $\langle \eta \rangle$ dependent second order term in the Taylor series expansion of $p^{\max}(\{\eta\})$. The coefficients have been obtained by second order fitting to numerically generated values for a hypercube sized $n = 8$. It is clearly visible that the coefficients are always greater than 2^{-n} . Another feature that is more suggestive on a linear scale is that the points between two steps seem to align into straight lines, with their slopes increasing with $\langle \eta \rangle$.

the mean deviation of $\{\eta\}$ as a distribution, and hence it is a well-defined statistical property of the random noise. In other words, as long as the second order Taylor expansion gives an acceptable approximation, the probability of success depends only on the two statistical properties of the noise $(\langle \eta \rangle, Q)$ and not on the particular values of $\{\eta\}$. We performed numerical studies up to rank $n = 10$ to investigate the behaviour of the coefficients B and C , and the validity of this assumption.

One of our first findings is that the introduction of errors in form of deviations from the uniform case improved the search efficiency in all the studied cases. A sample plot is displayed on Fig. 3 on which the relative improvement is compared to the uniform case in percentage. We observe that the general tendency is that for smaller values of $\langle \eta \rangle$ the improvement is larger, interrupted, however, by discontinuities. Our studies have shown that the number of discontinuous steps are proportional to the rank of hypercube. The figure shows the relative improvement for a system where $n = 9$ and the coefficients $\{\eta\}$ satisfy the condition $Q = 0.35$. An immediate consequence of this condition is that the possible values for $\langle \eta \rangle$ are restricted. We can also observe a particular spread of the curve formed by the data points, which we attribute to the higher order terms of the Taylor expansion.

We have also determined actual values of the second order Taylor coefficients by fitting to the numerical data. An example is provided on Fig. 4 for a system $n = 8$. We made attempts to minimize the effect of the spread caused by higher order terms by post selecting distributions $\{\eta\}$ with the lowest values for W . Nevertheless, this effect still affected the accuracy of the fitted parameters, however, the corresponding error bars on Fig. 4 are barely noticeable.

The resulting fitted coefficients are in accordance with

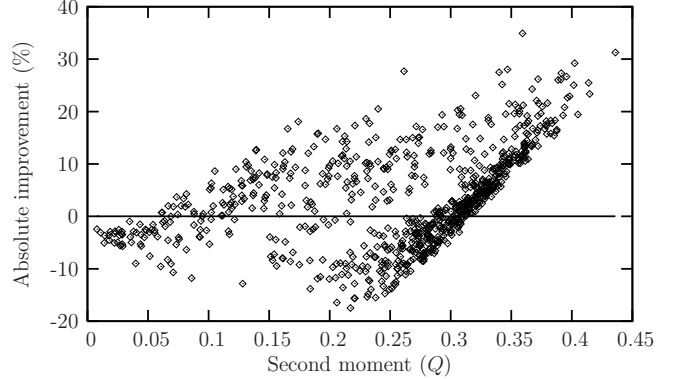


FIG. 5: Modification of success probability compared to the uniform case with the maximum transmission coefficient. Physically, the non-uniform case with $\{\eta\}$ can be obtained from the uniform with η_{\max} just by attenuation of optical paths. The second moment Q is used as a measure of deviation from the non-attenuated case. The vertical axis shows $[p^{\max}(\{\eta\}) - p^{\max}(\eta_{\max})]/p^{\max}(\eta_{\max})$ as a percentage. We observe a systematic improvement for higher values of Q . The plot corresponds to rank $n = 7$ and $\eta_{\max} = 0.996 \pm 0.001$.

our previous finding that deviations increase search efficiency. Furthermore, for all studied cases we found that $B \geq 2^{-n}$. We carried out further numerical studies involving third order coefficients and we found strong evidence that the lower bound

$$p^{\max}(\{\eta\}) \geq p^{\max}(\langle \eta \rangle) + 2^{-n}Q^2 \quad (37)$$

holds in general. The appeal of this lower bound is that it depends only on the size of the system $N = 2^n$, and the elementary statistical properties of the noise $(\langle \eta \rangle, Q)$.

So far in this section we were concerned with comparing the performance of the search algorithm suffering non-uniform losses with those suffering uniform loss with coefficient equal to the average of the non-uniform distribution. Another physically interesting question is how attenuation alone affects search efficiency. We can formulate this question using the notations above as follows. Consider a randomly generated distribution $\{\eta\}$ and compare the corresponding success probability with the one generated by a uniform distribution with transmission coefficient $\eta_{\max} = \max\{\eta\}$. We chose Q as a measure of how much an η_{\max} uniform distribution needs to be altered to obtain $\{\eta\}$. We carried out these comparisons using the previously generated samples up to ranks $n = 10$. A typical plot is presented on Fig. 5 as an example. It appears that as we start deviating from the original uniform distribution, an initial drop of efficiency is followed by a region where improvement shows some systematic increase. However, it is still an open question, whether it is really a general feature that for some values of Q the efficiency is always increased. On the other hand these plots provide clear evidence that for a significant number of cases the difference $p^{\max}(\{\eta\}) - p^{\max}(\eta_{\max})$ is positive. Hence, attenuation of certain optical paths

can lead to improvement of search efficiency. Knowing that the Grover coin is not the optimal choice for the search algorithm, this result would not be very surprising if the non-uniformity of losses were contributing a unitary modification. However, the corresponding loss operator is inherently non-unitary. Therefore, the behaviour, that in this case losses can improve search efficiency, is rather counter-intuitive.

V. PHASE ERRORS

The other type of errors that generally arise in optical multiport networks are due to optical path misalignments. Then the introduced errors come in the form of undesired random phases between the outputs. We may work in two regimes regarding these type of errors.

In a system where the undesired phases have such a slow drift that on the time scale of a single run of the algorithm their change is insignificant, we just have a modified version of the original walk. Of course, the repeated runs are expected to have different random phases, and this produces some interesting behaviour which we will consider here. On the other hand, if the noise is changing rapidly, different random phases are in effect at every iteration. A subset of the latter case has been studied in detail in Ref. [21] for uniform quantum walks with the Grover and Fourier coin.

Let F denote the operator introducing the phase shifts, and write it as

$$F(\{\varphi\}) = \sum_{d,x} e^{i\varphi_{dx}} |d, x\rangle\langle d, x|. \quad (38)$$

This operator is unitary, hence the step operator

$$U(\{\varphi\}) = U' F(\{\varphi\}), \quad (39)$$

that depends on the phases $\{\varphi_{dx} | d = 0..n-1, x = 0..2^n - 1\}$ is unitary as well. We could have defined the product in a different order, but it makes a difference only in the first step.

In case of slowly changing phases, we have a single set of parameters $\{\varphi\}$, and the evolution of the system over t steps can be written $|\psi_t(\{\varphi\})\rangle = U(\{\varphi\})^t |\psi_0\rangle$. Formally, the result after averaging can be written as

$$\varrho_{\text{out}} = \overline{|\psi_t(\{\varphi\})\rangle\langle\psi_t(\{\varphi\})|}^{\{\varphi\}}. \quad (40)$$

A reasonable model to characterize random configurations is to assume that the phases are distributed according to a Gaussian which is centered on the desired value, i.e. zero in this case, and has a given width which we denote by $\Delta\varphi$. The numerical results for calculating the time dependence of the success probability for several values of $\Delta\varphi$ are plotted on Fig. 6. The results have been obtained by calculating success probabilities for several different random phase configurations and taking their averages for every t .

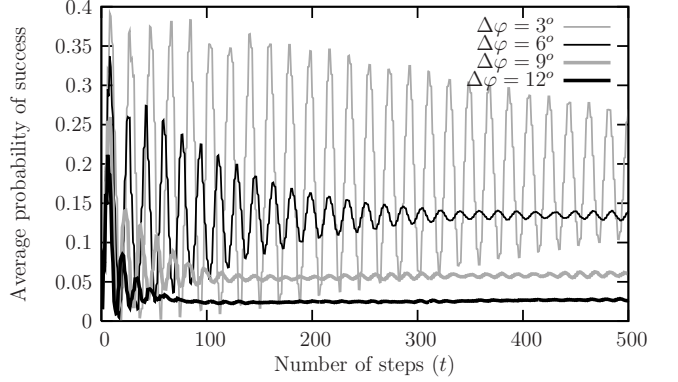


FIG. 6: The averaged (1000 samples) probability of measuring the target node, when $n = 6$ and $\Delta\varphi = 3^\circ, 6^\circ, 9^\circ, 12^\circ$. The tendency of the success probability to a constant, non-zero value can be observed on this numerically obtained plot. It is also observable that the larger widths give smaller asymptotic values.

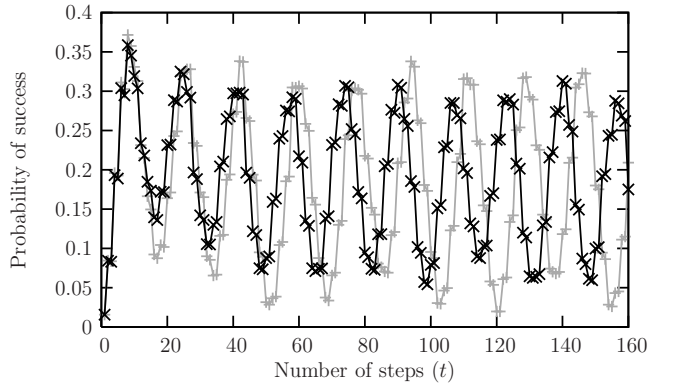


FIG. 7: Time dependence of success probabilities for two different phase configurations, numerically calculated for a system of rank $n = 6$. The difference in frequencies of the major oscillations is clearly observable for larger times.

By studying the repetition of the random phase configuration we come to several remarkable conclusions. First, the time evolution of the success probability tends (on a long time scale, $t \gg t_{\text{osc}}$) to a finite, non-zero constant value. Second, the early steps of the time evolution are characterized by damped oscillations reminding of a collapse. Third, the smaller the phase noise the larger is the long time stationary value to which the system evolves. We have plotted the stationary values obtained by numerical calculations, against the rank of the hypercube on Fig. 8.

The behaviour can be understood from the shape of the individual runs of the algorithm with the given random phase configurations. As it is observable on Fig. 7, the typical search algorithm oscillations differ slightly in the frequencies in dependence on the random phases chosen. Hence when such oscillations are summed up we get the typical collapse behaviour. Also, since these frequencies continuously fill up a band specified by the width of

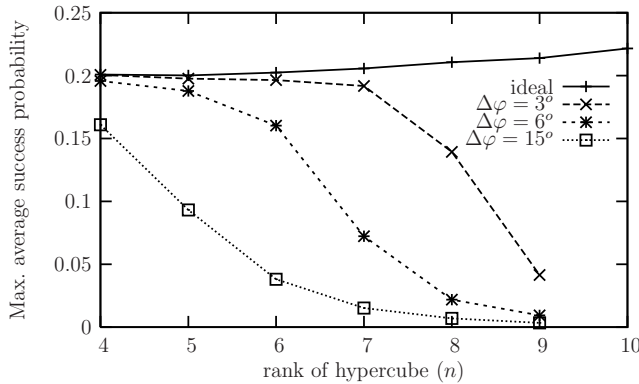


FIG. 8: The long time stationary values of the success probability (obtained by averaging over 1000 samples) against the size of the search space, for $\Delta\varphi = 0^\circ, 3^\circ, 6^\circ, 15^\circ$.

the Gaussian, we expect no revivals to happen later. For higher order hypercubes the success probability drops almost to zero for already very moderate phase errors, resembling a behaviour seen on Fig. 1.

VI. CONCLUSIONS

We analyzed QRWs used as search algorithms and analyzed the influence of several types of perturbations on their performance. Our main result for photon loss in the

SQRW search algorithm is that introduction of random direction dependence in the loss can significantly improve the search efficiency compared to uniform loss with the same average. In many cases, even the increase of losses in some random directions may improve the search efficiency. We could give an estimation of the lower bound for the search probability as a function of the average and variance of the randomly distributed direction dependent loss.

We analyzed the decrease of the search efficiency due to optical misalignment represented by direction dependent phase errors. In contrast to the previous studies we kept the phases fixed during each run of the search. As a result of this type of randomization we found out that the success rate does not drop to zero, but approaches a finite value. That behaviour stands in contrast to other types phase randomization considered in the literature [21]. The effect in its mechanism is reminiscent to exponential localization found in optical networks [23].

Acknowledgments

Support by the Czech and Hungarian Ministries of Education (CZ-2/2005), by MSMT LC 06002 and MSM 6840770039 and by the Hungarian Scientific Research Fund (T043287, T049234 and T068736) is acknowledged.

[1] Y. Aharonov, L. Davidovich, and N. Zagury, Phys. Rev. A **48**, 1687 (1993).
[2] J. Kempe, Contemp. Phys. **44**, 307 (2003).
[3] A. Ambainis, e-print quant-ph/0403120 (2004).
[4] L. Grover, in *Proceedings, 28th Annual ACM Symposium on the Theory of Computing (STOC)* (1996), pp. 212–219.
[5] N. Shenvi, J. Kempe, and K. B. Whaley, Phys. Rev. A **67**, 052307 (2003).
[6] S. Fujiwara, H. Osaki, I. M. Buluta, and S. Hasegawa, Phys. Rev. A **72**, 032329 (2005).
[7] B. C. Travaglione and G. J. Milburn, Phys. Rev. A **65**, 032310 (2002).
[8] J. Du, H. Li, X. Xu, M. Shi, J. Wu, X. Zhou, and R. Han, Phys. Rev. A **67**, 042316 (2003).
[9] C. A. Ryan, M. Laforest, J. C. Boileau, and R. Laflamme, Phys. Rev. A **72**, 062317 (2005).
[10] T. Di, M. Hillery, and M. S. Zubairy, Phys. Rev. A **70**, 032304 (2004).
[11] G. S. Agarwal and P. K. Pathak, Phys. Rev. A **72**, 033815 (2005).
[12] W. Dur, R. Raussendorf, V. M. Kendon, and H.-J. Briegel, Phys. Rev. A **66**, 052319 (2002).
[13] K. Eckert, J. Mompart, G. Birk, and M. Lewenstein, Phys. Rev. A **72**, 012327 (2005).
[14] E. Roldan and J. C. Soriano, J. Mod. Opt. **52**, 2649 (2005).
[15] P. L. Knight, E. Roldan, and J. E. Sipe, Optics Communications **227**, 147 (2003).
[16] M. Hillery, J. Bergou, and E. Feldman, Phys. Rev. A **68**, 032314 (2003).
[17] J. Košík and V. Bužek, Phys. Rev. A **71**, 012306 (2005).
[18] V. Kendon, e-print quant-ph/0606016 (2006).
[19] V. Kendon and B. Tregenna, Phys. Rev. A **67**, 042315 (2003).
[20] G. Alagic and A. Russell, Phys. Rev. A **72**, 062304 (2005).
[21] J. Košík, V. Bužek, and M. Hillery, Phys. Rev. A **74**, 022310 (2006).
[22] Y. Li, L. Ma, and J. Zhou, J. Phys. A: Math. Gen. **39**, 9309 (2006).
[23] P. Törmä, I. Jex, and W. P. Schleich, Phys. Rev. A **65**, 052110 (2002).